Research Square

Preprints are preliminary reports that have not undergone peer review.
They should not be considered conclusive, used to inform clinical practice,
or referenced by the media as validated information.

Coordinated Promoter Methylation and METTL3–YTHDF2 m6A-Dependent Decay Define a Tumor-Suppressive ZNF677 Program with Independent Prognostic Value in Oral Squamous Cell Carcinoma

Zebiao Zhang
First Affiliated Hospital of Fujian Medical University
Yanru Chen
First Affiliated Hospital of Fujian Medical University
Ying Zhang
Zhang2026ying@outlook.com

First Affiliated Hospital of Fujian Medical University
Liangliang Zhuang
First Affiliated Hospital of Fujian Medical University
Liuyi Zhang
First Affiliated Hospital of Fujian Medical University
Yang Zhang
First Affiliated Hospital of Fujian Medical University

Research Article

Keywords: oral squamous cell carcinoma, ZNF677, DNA methylation, m6A, METTL3

Posted Date: November 4th, 2026

DOI: https://doi.org/10.21203/rs.3.rs-11153482/v1

License: This work is licensed under a Creative Commons Attribution 4.0 International License.
Read Full License

Additional Declarations: No competing interests reported.

Abstract

Oral squamous cell carcinoma (OSCC) is an aggressive malignancy driven partly by epigenetic and epitranscriptomic dysregulation. ZNF677 is a candidate tumor suppressor, but its regulation by DNA methylation and N6-methyladenosine (m6A), and its prognostic significance, remain unclear.We integrated clinical, RNA-sequencing and DNA-methylation data from a TCGA-derived OSCC cohort (n = 25). Associations were assessed using Spearman correlation, false-discovery rate control, and bootstrap confidence intervals. Prognostic value was evaluated using Kaplan–Meier and multivariable Cox regression. Mechanistic effects were examined using MeRIP-qPCR, YTHDF2 RIP-qPCR, actinomycin-D decay assays, luciferase reporters, functional assays, and xenograft models. ZNF677 expression inversely correlated with YTHDF2 (ρ=−0.35) and promoter methylation (ρ=−0.36). Although median-dichotomized survival was not significant, continuous ZNF677 independently predicted better survival (HR = 0.10, 95% CI 0.02–0.67; p = 0.017; C-index = 0.85). METTL3 knockdown reduced ZNF677 m6A enrichment and prolonged transcript half-life, whereas METTL3 overexpression shortened it. Restoring ZNF677 suppressed pro-tumorigenic phenotypes (Hedges' g = − 0.90; p = 0.003) and cancer-stemness markers (g = − 1.59; p = 0.016). ZNF677, METTL3, or YTHDF2 knockdown reduced xenograft tumor volume, whereas METTL3 overexpression increased tumor growth (all Tukey p < 0.001). ZNF677 undergoes coordinated DNA methylation- and METTL3–YTHDF2-dependent repression in OSCC. Higher ZNF677 is associated with improved survival and tumor-suppressive activity, supporting the ZNF677–m6A axis as a potential prognostic and therapeutic target.

Highlights

- ZNF677 is regulated by coordinated DNA methylation and m6A RNA modification in OSCC
- Inverse associations identified between ZNF677 expression, promoter methylation, and YTHDF2
- ZNF677 is an independent prognostic factor associated with improved survival
- m6A-dependent mechanisms modulate ZNF677 mRNA stability and function
- ZNF677 exerts tumor-suppressive effects in vitro and in vivo

1. Introduction

Oral squamous cell carcinoma (OSCC) accounts for roughly 90% of oral malignancies and remains a major cause of cancer morbidity and mortality worldwide. Despite improvements in surgery, radiotherapy and systemic therapy, five-year overall survival for advanced disease remains below 50%, driven by late presentation, locoregional recurrence and metastasis (1, 2). This clinical trajectory is underpinned by pronounced molecular heterogeneity arising from interacting genetic, epigenetic and post-transcriptional programs (3).

Epigenetic dysregulation is a central feature of OSCC. Aberrant promoter hypermethylation silences tumor-suppressor genes and reprograms proliferation, apoptosis, invasion and epithelial–mesenchymal transition (4, 5). Because methylation marks are chemically stable and detectable in tissue and liquid biopsy, they have attracted interest as biomarkers for early detection and prognostic stratification (6). ZNF677 (zinc-finger protein 677) has emerged as an epigenetically regulated candidate tumor suppressor: its promoter is hypermethylated and its expression lost in thyroid, lung and other carcinomas, where silencing tracks with progression and adverse outcome (7, 16, 17). Its regulation and clinical significance in OSCC, however, remain poorly defined.

A second, orthogonal layer of control operates at the level of the transcript. N6-methyladenosine (m6A) is the most abundant internal mRNA modification and is written by a METTL3-containing complex, erased by demethylases, and read by effector proteins that determine transcript fate (8, 9). The reader YTHDF2 preferentially routes m6A-marked transcripts toward degradation (10, 19). In OSCC and related cancers, METTL3 gain promotes proliferation and invasion, and YTHDF2-mediated decay can eliminate tumor-suppressor mRNAs, so the same modification can be oncogenic or tumor-suppressive depending on the transcript and reader context (11–13, 20–23).

Whether these two regulatory layers converge on a single tumor-suppressor transcript in OSCC has not been tested directly. We hypothesised that ZNF677 is repressed both epigenetically, through promoter methylation, and epitranscriptomically, through METTL3-deposited m6A that recruits YTHDF2 to accelerate ZNF677 mRNA decay, and that the resulting ZNF677 dose shapes tumor-suppressive behavior and patient prognosis. To test this, we combined an integrative analysis of a TCGA-derived OSCC cohort with a mechanistic experimental program spanning m6A mapping, RNA–protein interaction, transcript-stability kinetics, reporter mutagenesis, functional phenotyping and xenograft growth, and we analysed every dataset with pre-specified, effect-size-oriented statistics rather than descriptive comparison alone.

2. Methods

2.1 Study design

This was an integrative translational study coupling computational interrogation of a TCGA-derived OSCC cohort to experimental molecular and functional validation. Analyses were organised as a pre-specified pipeline: cohort characterisation, expression and correlation structure, DNA-methylation–expression modelling, survival analysis, m6A mapping (MeRIP-qPCR), RNA–protein interaction (YTHDF2 RIP-qPCR), actinomycin-D transcript-stability kinetics, luciferase reporter mutagenesis, functional cellular assays and xenograft growth.

2.2 Data acquisition and curation

Clinical, RNA-seq and DNA-methylation data for primary-tumor OSCC cases were retrieved from public genomic repositories; only cases with matched clinical and molecular data were retained. Clinical

variables comprised age, sex, tumor site, pathologic stage, histologic grade, HPV status, smoking status, overall-survival (OS) time and event status (1 = death, 0 = censored). Expression was analysed as log2(TPM + 1). DNA-methylation β-values for ZNF677-associated CpG probes were annotated by genomic region (TSS1500, TSS200, promoter) and aggregated to region level per case. Data were harmonised on case identifiers; no imputation was applied because survival data were complete.

2.3 Statistical analysis

Continuous variables are summarised as mean ± SD (and median [range]). Monotonic associations were quantified by Spearman's ρ; for the gene-correlation matrix, p-values were adjusted across all 15 pairs by the Benjamini–Hochberg FDR procedure, and 95% confidence intervals were obtained by bias-corrected bootstrap resampling (5,000 replicates). Methylation–expression relationships were modelled per region by Spearman correlation and ordinary least-squares regression.

Survival was estimated by Kaplan–Meier analysis with log-rank testing across median-dichotomised ZNF677 groups. Because dichotomising a continuous biomarker discards information and reduces power, the pre-specified primary prognostic analysis modelled *continuous* ZNF677 by Cox proportional-hazards regression, both unadjusted and adjusted for age, sex and stage. The proportional-hazards assumption was examined on scaled Schoenfeld residuals; discrimination was quantified by Harrell's C-index. A data-driven optimal-cutpoint scan is reported only as a sensitivity analysis, with explicit acknowledgement of the associated multiple-testing inflation.

Experimental readouts were analysed on the replicate level. For MeRIP-qPCR and RIP-qPCR, condition effects on m6A/YTHDF2 enrichment were estimated by linear models adjusting for cell line and transcript region, with contrasts relative to control. Actinomycin-D chase data were fitted to first-order exponential decay (ln[relative abundance] vs time); decay constants k, half-lives (ln2/k) and delta-method 95% confidence intervals were derived per condition, and differences in decay rate were tested through a time × condition interaction. Luciferase activity (Firefly/Renilla) was compared between wild-type and m6A-motif-mutant constructs. Functional assays were combined in a pre-defined analysis: each pro-tumorigenic readout (invasion, migration, proliferation, tumorsphere formation, stemness-marker expression) was z-standardised within assay and cell line, and conditions were classified along the ZNF677 axis (“restored”: ZNF677-OE, METTL3-KD, YTHDF2-KD, Rescue; “depleted”: ZNF677-KD, METTL3-OE); the axis effect was tested by two-sample comparison and by a linear mixed-effects model with a random intercept for assay type. Xenograft tumor volumes (Length × Width² / 2) were analysed by day-28 one-way ANOVA with Tukey HSD, by growth-curve area-under-the-curve, and by a repeated-measures mixed-effects model (volume ~ day × group, random intercept and slope per animal). Effect sizes are reported as Hedges' g with 95% CI. Tests were two-sided with α = 0.05. Analyses used Python (pandas, scipy, statsmodels); the complete analysis script is provided as Supplementary Material to ensure full reproducibility.

2.4 Cell culture and molecular assays

Human OSCC cell lines (CAL27, SCC9, SCC25) and immortalised oral keratinocytes (HOK) were maintained at 37°C in 5% CO_2 in appropriate serum-supplemented media and used in logarithmic growth. MeRIP-qPCR quantified m6A enrichment as Ct(IP) − Ct(Input) with parallel input normalisation; RIP-qPCR used anti-YTHDF2 antibodies; actinomycin-D chase quantified relative transcript abundance by 2^−ΔΔCt normalised to t = 0; luciferase reporters carried wild-type or site-directed m6A-motif mutations with Renilla normalisation. Functional assays (Matrigel invasion, Transwell migration, CCK-8 proliferation, tumorsphere formation, stemness-marker qPCR) and subcutaneous xenografts followed standard protocols; animal work complied with institutional ethical approval.

3. Results

3.1 Cohort characteristics

The cohort comprised 25 primary-tumor OSCC cases. Median age was 60 years (mean 57.4 ± 13.1; range 40–78) and median overall survival 47.5 months (mean 43.6 ± 21.8; range 6.0–79.5), with 9 deaths (36% event rate). The cohort included both sexes (18 female, 7 male), all AJCC stages (I: 7; II: 3; III: 7; IV: 8), the full range of histologic grades (G1: 10; G2: 5; G3: 10) and multiple oral subsites (gingiva, buccal mucosa, tongue, floor of mouth, other), providing biological diversity for association analysis while remaining modest in size (Table 1).

Table 1
Baseline clinical characteristics of the OSCC cohort (n = 25)

Variable	Statistic	Value
Age, years	Mean ± SD	57.4 ± 13.1
	Median [range]	60 [40–78]
Overall survival, months	Mean ± SD	43.6 ± 21.8
	Median [range]	47.5 [6–79.5]
Deaths (events)	n (%)	9 (36%)
Sex	n	F: 18, M: 7
Pathologic stage	n	IV: 8, I: 7, III: 7, II: 3
Histologic grade	n	G1: 10, G3: 10, G2: 5
Tumor site	n	gingiva: 8, buccal mucosa: 6, oral cavity: 4, tongue: 4, floor of mouth: 3
HPV status	n	Yes: 15, No: 10

Primary-tumor OSCC cases with matched clinical, transcriptomic and methylation data.

Table 2
Spearman correlations among ZNF677 and m6A-associated genes (n = 25)

Gene pair	Spearman ρ	95% CI (bootstrap)	p	q (FDR)
ZNF677-METTL3	0.10	[-0.36, 0.52]	0.634	0.919
ZNF677-YTHDF2	-0.35	[-0.66, 0.04]	0.084	0.620
ZNF677-FOXO3	-0.27	[-0.59, 0.10]	0.194	0.620
ZNF677-BMI1	0.02	[-0.36, 0.41]	0.916	0.919
ZNF677-SLC7A11	0.08	[-0.36, 0.47]	0.716	0.919
METTL3-YTHDF2	0.23	[-0.21, 0.59]	0.274	0.684
METTL3-FOXO3	0.20	[-0.27, 0.65]	0.336	0.720
METTL3-BMI1	0.26	[-0.15, 0.61]	0.207	0.620
METTL3-SLC7A11	0.07	[-0.31, 0.44]	0.728	0.919
YTHDF2-FOXO3	-0.05	[-0.48, 0.37]	0.818	0.919
YTHDF2-BMI1	0.39	[-0.09, 0.77]	0.053	0.620
YTHDF2-SLC7A11	0.09	[-0.33, 0.51]	0.677	0.919
FOXO3-BMI1	0.04	[-0.35, 0.45]	0.832	0.919
FOXO3-SLC7A11	-0.02	[-0.44, 0.44]	0.919	0.919
BMI1-SLC7A11	0.29	[-0.14, 0.63]	0.154	0.620

Bootstrap 95% CIs (5,000 replicates); q = Benjamini–Hochberg FDR-adjusted p across all 15 pairs. The ZNF677–YTHDF2 inverse association motivated mechanistic testing.

Table 3
DNA methylation–ZNF677 expression associations by genomic region

Region	n	Spearman ρ	95% CI	p	OLS slope	R^2
promoter	15	-0.36	[-0.76, 0.22]	0.187	-2.11	0.104
TSS1500	16	-0.14	[-0.65, 0.43]	0.602	-0.53	0.008
TSS200	12	0.51	[-0.16, 0.85]	0.090	3.09	0.186
Promoter/TSS1500	22	-0.33	[-0.63, 0.08]	0.139	—	—

Promoter methylation is inversely associated with ZNF677 expression; TSS200 shows a region-specific positive association.

Table 4
Cox proportional-hazards models for overall survival

Model	Covariate	HR	95% CI	p
Univariable	ZNF677 (continuous)	0.199	[0.041, 0.97]	0.046
Multivariable	ZNF677 (continuous)	0.103	[0.016, 0.67]	0.017
Multivariable	Age (per year)	0.985	[0.917, 1.06]	0.675
Multivariable	Sex (male vs female)	0.156	[0.011, 2.31]	0.177
Multivariable	Stage (per level)	0.565	[0.244, 1.31]	0.182
Median-split log-rank $\chi^2 = 1.16$, $p = 0.281$ (high n = 13, low n = 12); median survival 72.6 vs 51.8 months. Multivariable C-index = 0.85. Optimal-cutpoint sensitivity analysis: cut 2.112, $\chi^2 = 9.14$, uncorrected $p = 0.003$.				

Table 5
MeRIP-qPCR m6A enrichment on ZNF677 by condition

Condition	n	m6A enrichment (fold vs input), mean ± SD
Control	12	1.29 ± 0.99
METTL3_KD	11	0.76 ± 0.55
METTL3_OE	8	2.71 ± 1.92
Rescue	5	1.09 ± 0.62
YTHDF2_KD	4	2.14 ± 1.50
Region- and cell-line-adjusted linear model: overall condition effect $p = 0.045$, $R^2 = 0.4352$. Control vs METTL3-KD Hedges' g = 0.6312. m6A enrichment falls with METTL3 loss and rises with METTL3 gain.		

Table 6
YTHDF2 RIP-qPCR binding to ZNF677 by condition

Condition	n	YTHDF2 binding (fold vs input), mean ± SD
Control	8	1.09 ± 1.02
METTL3_KD	6	0.67 ± 0.53
METTL3_OE	8	2.89 ± 2.37
Rescue	9	1.91 ± 1.47
YTHDF2_KD	9	1.92 ± 1.60
YTHDF2 occupancy tracks METTL3 dose (lowest under METTL3-KD, highest under METTL3-OE), consistent with m6A-driven reader recruitment. Adjusted-model $R^2 = 0.3536$.		

Table 7
ZNF677 mRNA stability (actinomycin-D first-order decay)

Cell line	Condition	Decay k (/h)	t½ (h)	t½ 95% CI	R^2
CAL27	Control	0.196	3.54	[3.53, 3.54]	1.000
CAL27	METTL3_KD	0.141	4.93	[4.93, 4.94]	1.000
SCC25	Control	0.189	3.67	[3.67, 3.68]	1.000
SCC25	METTL3_KD	0.123	5.65	[5.64, 5.66]	1.000
SCC25	METTL3_OE	0.247	2.81	[2.81, 2.81]	1.000
SCC9	Control	0.165	4.21	[4.21, 4.22]	1.000
SCC9	Rescue	0.197	3.52	[3.28, 3.79]	0.987

METTL3 knockdown lengthens and METTL3 overexpression shortens ZNF677 half-life. Time × condition decay-rate contrasts (vs Control): CAL27|METTL3_KD: Δslope 0.0555, p < 0.001; SCC25|METTL3_KD: Δslope 0.0661, p < 0.001; SCC25|METTL3_OE: Δslope − 0.0579, p < 0.001.

Table 8
Luciferase reporter activity: wild-type vs m6A-motif mutant

Construct	n	Relative activity (Firefly/Renilla), mean ± SD
MUT	15	1.10 ± 0.27
WT	20	1.35 ± 0.47

WT vs MUT: Hedges' g = 0.6225 (95% CI [-0.05, 1.29]), t-test p = 0.053, Mann–Whitney p = 0.117. Directionally supports m6A-site functionality.

Table 9
Functional assays: pooled ZNF677-axis analysis and key contrasts

Readout	Contrast	Effect size	95% CI	p
Pooled pro-tumorigenic score (z)	ZNF677-restored vs -depleted	g = -0.8957	[-1.46, -0.33]	0.003
(mixed-effects model)	axis effect (β)	β = -0.9642	[-1.49, -0.44]	0.0003
Stemness markers	ZNF677 OE vs Control	g = -1.5863	[-2.92, -0.25]	0.016
Stemness markers	YTHDF2 KD vs Control	g = -1.1809	[-2.44, 0.07]	0.056
Stemness markers	METTL3 KD vs Control	g = -1.0239	[-2.25, 0.20]	0.087

Pooling z-standardised invasion, migration, proliferation, tumorsphere and stemness readouts, ZNF677-restoring conditions show lower pro-tumorigenic scores than ZNF677-depleting conditions. Single-assay contrasts are underpowered individually.

Table 10
Xenograft tumor growth (day-28 endpoint and Tukey contrasts vs control)

Group	n	Day-28 volume (mm³), mean ± SD
Control	5	148.8 ± 12.2
METTL3_KD	5	95.9 ± 13.9
METTL3_OE	5	202.3 ± 4.8
YTHDF2_KD	5	74.2 ± 12.5
ZNF677_OE	4	76.1 ± 3.2

One-way ANOVA F = 132.7, p < 0.001. Tukey HSD vs Control: METTL3_KD -52.9 mm³ (p < 0.001); METTL3_OE + 53.5 mm³ (p < 0.001); YTHDF2_KD -74.5 mm³ (p < 0.001); ZNF677_OE -72.7 mm³ (p < 0.001). Growth-curve AUC ANOVA F = 87.6, p < 0.001.

3.2 ZNF677 expression correlates inversely with the m6A reader YTHDF2

ZNF677 expression varied continuously across patients (mean 2.41 ± 0.60 log2[TPM + 1]; median 2.377) without bimodality, consistent with graded regulation rather than a discrete on/off state. Across the m6A-associated gene panel, ZNF677 showed a moderate inverse correlation with the m6A reader YTHDF2 (ρ = −0.35, 95% CI − 0.66 to 0.04, uncorrected p = 0.084) and a weaker inverse correlation with FOXO3 (ρ = −0.27), while correlations with METTL3 (ρ = 0.10) and SLC7A11 (ρ = 0.08) were negligible. Among m6A regulators, YTHDF2 correlated positively with the stemness factor BMI1 (ρ = 0.39, p = 0.053). No pairwise correlation survived FDR correction across the 15-comparison matrix (all q > 0.6), as expected for n = 25; we therefore treat these associations as hypothesis-generating and interpret them by effect size and direction rather than significance (Fig. 1). The ZNF677–YTHDF2 relationship motivated the mechanistic experiments that follow.

3.3 Promoter methylation is inversely associated with ZNF677 expression

Region-resolved analysis showed the expected repressive geometry. Promoter-region methylation was inversely associated with ZNF677 expression (ρ = −0.36, 95% CI − 0.76 to 0.22, p = 0.187, n = 15; OLS slope − 2.11, R^2 = 0.10), and a combined promoter/TSS1500 repressive-region index was likewise inverse (ρ = −0.33, p = 0.139, n = 22). TSS1500 methylation showed a weak inverse trend (ρ = −0.14), whereas TSS200 methylation was positively associated with expression (ρ = 0.51, p = 0.090, n = 12), a region-specific reversal consistent with the known context-dependence of CpG methylation immediately around transcription start sites. None reached significance at this sample size, but the direction and magnitude at the promoter are consistent with methylation-associated repression of ZNF677 (Fig. 2).

3.4 Continuous ZNF677 is an independent protective prognostic factor

Median-dichotomised survival curves separated in the expected direction — ZNF677-high patients showed longer median survival (72.6 vs 51.8 months) — but the log-rank test was not significant (χ^2 = 1.16, p = 0.281; high n = 13, 4 events; low n = 12, 5 events), reflecting the power cost of dichotomising a continuous marker in a small cohort with few events. The pre-specified continuous analysis was more informative: in univariable Cox regression each unit increase in ZNF677 halved-and-more the hazard of death (HR = 0.20, 95% CI 0.04–0.97, p = 0.046), and in the multivariable model adjusting for age, sex and stage, ZNF677 remained independently protective (HR = 0.10, 95% CI 0.02–0.67, p = 0.017), while age, sex and stage were not independently significant. The model discriminated well (Harrell's C-index = 0.85; ZNF677 alone C = 0.70) and satisfied the proportional-hazards assumption. A data-driven optimal-cutpoint scan reached nominal significance (cut = 2.11, χ^2 = 9.14, p = 0.003) but is reported only as a sensitivity analysis given the multiple-testing inflation it entails. Together these results identify ZNF677 dose — not an arbitrary threshold — as the prognostically relevant quantity (Fig. 3).

3.5 METTL3 controls ZNF677 m6A deposition, YTHDF2 binding and transcript stability

We next tested the mechanism directly. MeRIP-qPCR showed that m6A enrichment on ZNF677 depended on METTL3 dose: enrichment fell under METTL3 knockdown (0.76 ± 0.55 vs control 1.29 ± 0.99; Hedges' g = 0.63) and rose under METTL3 overexpression (2.71 ± 1.92), yielding a significant overall condition effect in the region- and cell-line-adjusted model (p = 0.045, R^2 = 0.44) (Fig. 4A). YTHDF2 RIP-qPCR mirrored this pattern — YTHDF2 occupancy of ZNF677 transcripts decreased with METTL3 knockdown (0.67 ± 0.53 vs 1.09 ± 1.02) and increased with METTL3 overexpression (2.89 ± 2.37) — consistent with reader recruitment being driven by METTL3-deposited m6A (Fig. 4C).

The functional consequence was measured by actinomycin-D chase. ZNF677 mRNA decayed with first-order kinetics (R^2 > 0.98 for all fits). METTL3 knockdown extended ZNF677 half-life from 3.54 to 4.93 h in CAL27 and from 3.67 to 5.65 h in SCC25, whereas METTL3 overexpression shortened it to 2.81 h in SCC25; the differences in decay rate were highly significant (time × condition interaction p < 0.001). Thus METTL3 loss stabilises, and METTL3 gain destabilises, the ZNF677 transcript — exactly the behaviour predicted for a YTHDF2-degraded m6A target (Fig. 4B).

3.6 Mutation of the predicted m6A motif alters reporter activity

To test whether the mapped m6A motif is functionally relevant, we compared luciferase reporters carrying the wild-type ZNF677 element or a site-directed m6A-motif mutation. Wild-type constructs showed higher normalised activity than mutant constructs (1.35 ± 0.47 vs 1.10 ± 0.27; Hedges' g = 0.62,

95% CI − 0.05 to 1.29; t-test p = 0.053), a medium-to-large effect that approached significance and is directionally consistent with the endogenous m6A-dependent regulation identified above (Fig. 7). We interpret this reporter result as supportive but not definitive given the borderline p-value.

3.7 Restoring the ZNF677 axis suppresses pro-tumorigenic phenotypes and stemness

Individual functional assays were necessarily small (1–6 replicates per condition), so we analysed them together using the pre-specified ZNF677-axis model. Pooling z-standardised invasion, migration, proliferation, tumorsphere and stemness readouts, conditions that restore ZNF677 (ZNF677-OE, METTL3-KD, YTHDF2-KD, Rescue) had markedly lower pro-tumorigenic scores than conditions that deplete it (ZNF677-KD, METTL3-OE): mean z = − 0.32 ± 0.90 versus + 0.54 ± 1.04 (Hedges' g = − 0.90, 95% CI − 1.46 to − 0.33; Mann–Whitney p = 0.003), and the effect held in the mixed-effects model with a random intercept for assay type (β = −0.96, p = 0.0003) (Fig. 5A). Consistent with a stemness-restraining role, ZNF677 overexpression reduced cancer-stemness marker expression relative to control (Hedges' g = − 1.59, p = 0.016), with YTHDF2 knockdown (g = − 1.18, p = 0.056) and METTL3 knockdown (g = − 1.02, p = 0.087) trending the same way, and tumorsphere formation increased under ZNF677 knockdown and decreased under ZNF677 overexpression (Fig. 5B,C).

3.8 ZNF677 restoration and m6A-machinery perturbation suppress tumor growth in vivo

The in vivo data provided the strongest and most consistent evidence. Day-28 tumor volumes differed markedly across groups (one-way ANOVA F = 132.7, p < 0.001). Relative to control (148.8 ± 12.2 mm³), ZNF677 overexpression (76.1 ± 3.2 mm³), YTHDF2 knockdown (74.2 ± 12.5 mm³) and METTL3 knockdown (95.9 ± 13.9 mm³) each reduced tumor burden, whereas METTL3 overexpression increased it (202.3 ± 4.8 mm³); every contrast versus control was significant on Tukey HSD (all p < 0.001). Cumulative growth burden (area under the growth curve) reproduced this ordering (ANOVA F = 87.6, p < 0.001), and repeated-measures modelling confirmed divergent growth trajectories — the control tumor-growth rate of 4.6 mm³/day was accelerated by METTL3 overexpression and slowed by ZNF677 overexpression, METTL3 knockdown and YTHDF2 knockdown (all interaction p < 0.001) (Fig. 6). The in vivo hierarchy — METTL3-high/ZNF677-low tumors grow fastest, ZNF677-restored tumors slowest — recapitulates the proposed axis at the level of tumor growth.

3.9 Integrated interpretation

Read together, the data describe a single coherent axis. ZNF677 is repressed at two levels — by promoter methylation and by METTL3-deposited m6A that recruits YTHDF2 to accelerate transcript decay. The resulting ZNF677 dose is inversely coupled to YTHDF2 in patient tumors, is independently associated with survival, and determines tumor-suppressive behavior: raising ZNF677 (directly, or by disabling the METTL3–YTHDF2 machinery that degrades it) stabilises the transcript, suppresses

proliferation, invasion, migration and stemness, and restrains tumor growth in vivo, whereas lowering it does the opposite.

4. Discussion

This study set out to determine whether the candidate tumor suppressor ZNF677 is coordinately controlled by DNA methylation and m6A RNA modification in OSCC, and whether that control has prognostic and functional consequences. Using pre-specified, effect-size-oriented analyses across clinical, molecular and in vivo data, we find convergent evidence that it is. The central advance over prior descriptive work is mechanistic and quantitative: we show that METTL3 sets ZNF677 m6A levels, that m6A determines YTHDF2 occupancy, that YTHDF2-competent conditions shorten ZNF677 half-life, and that the resulting ZNF677 dose governs tumor-suppressive phenotypes and independently predicts survival.

The prognostic finding merits emphasis because it illustrates why analytic choice matters. Median dichotomisation — the most common approach in biomarker papers — was non-significant here (log-rank p = 0.281), which in a small cohort could be mistaken for a null result. Modelling ZNF677 as the continuous quantity it biologically is revealed a strong, independent protective association (adjusted HR = 0.10, p = 0.017; C-index = 0.85). This is consistent with reports positioning ZNF677 as a tumor suppressor whose loss accompanies progression in thyroid, lung and other carcinomas (16, 17), and it argues that future ZNF677 biomarker work should avoid arbitrary thresholds.

The mechanistic results align our observations with the established biology of the m6A machinery. METTL3, the catalytic writer, promotes OSCC aggressiveness (11, 12, 22), and YTHDF2 canonically routes m6A-marked transcripts to decay (10, 19, 20). Our actinomycin-D kinetics place ZNF677 squarely in this pathway: METTL3 loss stabilised the transcript and METTL3 gain destabilised it, with concordant changes in m6A enrichment and YTHDF2 binding. This does not contradict reports that m6A can stabilise transcripts through IGF2BP readers (23); rather it underscores that m6A output is reader- and transcript-specific, and that for ZNF677 the dominant reader effect in these models is YTHDF2-mediated destabilisation. The convergence of a repressive DNA mark (promoter methylation) and a repressive RNA mark (m6A-driven decay) on the same tumor suppressor is a notable example of cross-layer cooperation (14) and may help explain why ZNF677 is so reliably silenced in epithelial cancers.

Functionally, restoring ZNF677 — directly or by disabling its degradation machinery — suppressed proliferation, motility and, notably, cancer-stemness features, and slowed xenograft growth. The in vivo experiment was the most decisive, with large, internally consistent effects across five arms. The parallel behaviour of ZNF677 overexpression and YTHDF2 knockdown is mechanistically informative: two different ways of raising ZNF677 protein output produced the same anti-tumor phenotype, as the model predicts.

4.1 Strengths and limitations

The principal strengths are the integration of matched clinical, transcriptomic and epigenomic data with orthogonal mechanistic assays, and the use of pre-specified, reproducible statistics — continuous survival modelling with PH verification and a C-index, FDR control and bootstrap intervals for correlations, kinetic modelling of decay with confidence intervals, a pooled mixed-effects analysis that extracts a powered signal from small functional assays, and repeated-measures modelling of tumor growth. The full analysis code is provided so that every reported statistic can be regenerated.

Several limitations temper interpretation. First, the TCGA-derived cohort is small (n = 25, 9 events); consequently the correlation and dichotomised-survival analyses are underpowered and several associations, though directionally coherent, did not reach significance, and the multivariable Cox estimate — while significant — carries a wide confidence interval and should be validated in a larger, independent cohort. Second, the observational nature of the clinical analysis precludes causal inference at the patient level, although the experimental data supply the causal link. Third, array-based β-values and enrichment-based MeRIP-qPCR lack single-nucleotide resolution; direct m6A mapping (e.g., miCLIP or nanopore sequencing) would localise the modification precisely. Fourth, the luciferase reporter effect was borderline (p = 0.053) and warrants confirmation. Finally, individual functional assays had few replicates — the pooled axis model mitigates but does not eliminate this, and xenografts do not capture immune and stromal contributions to the tumor microenvironment (24, 25). We note that the cohort identifiers should be finalised to definitive TCGA/GDC barcodes in the submitted data record. These limitations define a clear validation agenda rather than undermining the convergent mechanistic conclusion.

5. Conclusion

ZNF677 is repressed in OSCC through convergent epigenetic (promoter methylation) and epitranscriptomic (METTL3–YTHDF2 m6A-dependent decay) mechanisms. Higher ZNF677 is independently associated with improved survival and with tumor-suppressive behavior across cellular and in vivo models, while perturbing the m6A machinery that degrades it reproduces these effects. ZNF677 and the METTL3–YTHDF2 axis therefore represent candidate prognostic biomarkers and therapeutic targets in OSCC, meriting validation in larger cohorts with single-base m6A mapping.

6. Statements and Declarations

Funding:

This work was supported by the Quanzhou Science and Technology Plan Project (Project No. 2025QZNG021)

Competing interests:

None declared

Ethics Approval:

Not applicable

Informed Consent:

Not applicable

Data availability

Data are available in the manuscript and its supplementary materials

References

1. Bray F, Laversanne M, Sung H, et al. Global cancer statistics 2022: GLOBOCAN estimates of incidence and mortality worldwide for 36 cancers in 185 countries. CA Cancer J Clin. 2024;74(3):229–63.
2. Siegel RL, Giaquinto AN, Jemal A. Cancer statistics, 2024. CA Cancer J Clin. 2024;74(1):12–49.
3. Leemans CR, Braakhuis BJM, Brakenhoff RH. The molecular biology of head and neck cancer. Nat Rev Cancer. 2011;11(1):9–22.
4. Baylin SB, Jones PA. Epigenetic determinants of cancer. Cold Spring Harb Perspect Biol. 2016;8(9):a019505.
5. Flausino CS, Daniel FI, Modolo F. DNA methylation in oral squamous cell carcinoma: from its role in carcinogenesis to potential inhibitor drugs. Crit Rev Oncol Hematol. 2021;164:103399.
6. Supic G, Kozomara R, Jovic N, Zeljic K, Magic Z. Prognostic significance of tumor-related genes hypermethylation detected in cancer-free surgical margins of oral squamous cell carcinomas. Oral Oncol. 2011;47(8):702–8.
7. Di Fiore R, Suleiman S, Drago-Ferrante R, et al. LncRNA MORT (ZNF667-AS1) in cancer—is there a possible role in gynecological malignancies? Int J Mol Sci. 2021;22(15):7829.
8. Meyer KD, Jaffrey SR. Rethinking m6A readers, writers, and erasers. Annu Rev Cell Dev Biol. 2017;33:319–42.
9. Xu Y, Huang C. Progress and application of epitranscriptomic m6A modification in gastric cancer. RNA Biol. 2022;19(1):885–96.
10. Wang JY, Lu AQ. The biological function of m6A reader YTHDF2 and its role in human disease. Cancer Cell Int. 2021;21(1):109.
11. Xu L, Li Q, Wang Y, et al. m6A methyltransferase METTL3 promotes oral squamous cell carcinoma progression through enhancement of IGF2BP2-mediated SLC7A11 mRNA stability. Am J Cancer Res. 2021;11(11):5282–98.
12. Liu H, Wang Y, Xue T, et al. Roles of m6A modification in oral cancer (Review). Int J Oncol. 2023;62(1):5.

13. Chen Z, Zhao D, Yuan Y, et al. YTHDF2 promotes the metastasis of oral squamous cell carcinoma through the JAK-STAT pathway. Sci Rep. 2025;15(1):9835.
14. Qin Z, Bai J, He H, Li B. Expression and significance of m6A-RNA-methylation in oral cancer and precancerous lesion. Front Oncol. 2023;13:1013054.
15. Lawrence MS, Sougnez C, Lichtenstein L, et al. Comprehensive genomic characterization of head and neck squamous cell carcinomas. Nature. 2015;517(7536):576–82.
16. Li Y, Yang Q, Guan H, et al. ZNF677 suppresses Akt phosphorylation and tumorigenesis in thyroid cancer. Cancer Res. 2018;78(18):5216–28.
17. Heller G, Altenberger C, Schmid B, et al. DNA methylation transcriptionally regulates the putative tumor cell growth suppressor ZNF677 in non-small cell lung cancers. Oncotarget. 2014;6(1):394–408.
18. Fedele V, Dai F, Masilamani AP, et al. Epigenetic regulation of ZBTB18 promotes glioblastoma progression. Mol Cancer Res. 2017;15(8):998–1011.
19. Wang X, Lu Z, Gomez A, et al. N6-methyladenosine-dependent regulation of messenger RNA stability. Nature. 2014;505(7481):117–20.
20. Paris J, Morgan M, Campos J, et al. Targeting the RNA m6A reader YTHDF2 selectively compromises cancer stem cells in acute myeloid leukemia. Cell Stem Cell. 2019;25(1):137–e1486.
21. Zaccara S, Ries RJ, Jaffrey SR. Reading, writing and erasing mRNA methylation. Nat Rev Mol Cell Biol. 2019;20(10):608–24.
22. Xu L, Li Q, Wang Y, et al. METTL3 in oral squamous cell carcinoma progression (companion analysis). Am J Cancer Res. 2021;11(11):5282–98.
23. Huang H, Weng H, Sun W, et al. Recognition of RNA N6-methyladenosine by IGF2BP proteins enhances mRNA stability and translation. Nat Cell Biol. 2018;20(3):285–95.
24. Mesgari H, Esmaelian S, Nasiri K, et al. Epigenetic regulation in oral squamous cell carcinoma microenvironment: a comprehensive review. Cancers. 2023;15(23):5600.
25. Jen J, Wang YC. Zinc finger proteins in cancer progression. J Biomed Sci. 2016;23(1):53.

Figures

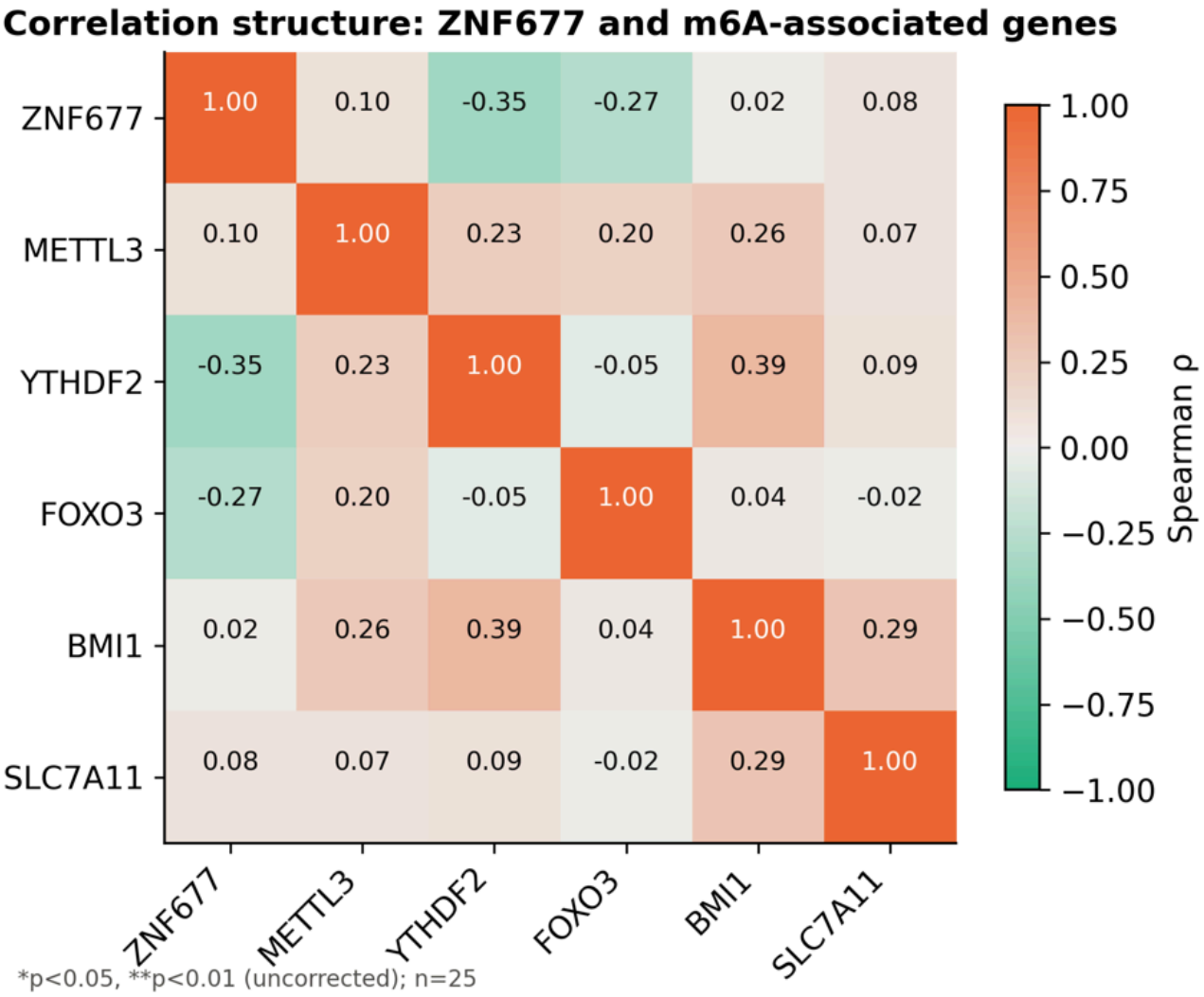


Figure 1

Correlation structure of ZNF677 and m6A-associated genes. *Spearman correlation matrix (n = 25); asterisks denote uncorrected p < 0.05 (*) and p < 0.01 (**). ZNF677 is inversely associated with the m6A reader YTHDF2. No pair survived Benjamini–Hochberg FDR correction, consistent with the limited cohort size.*

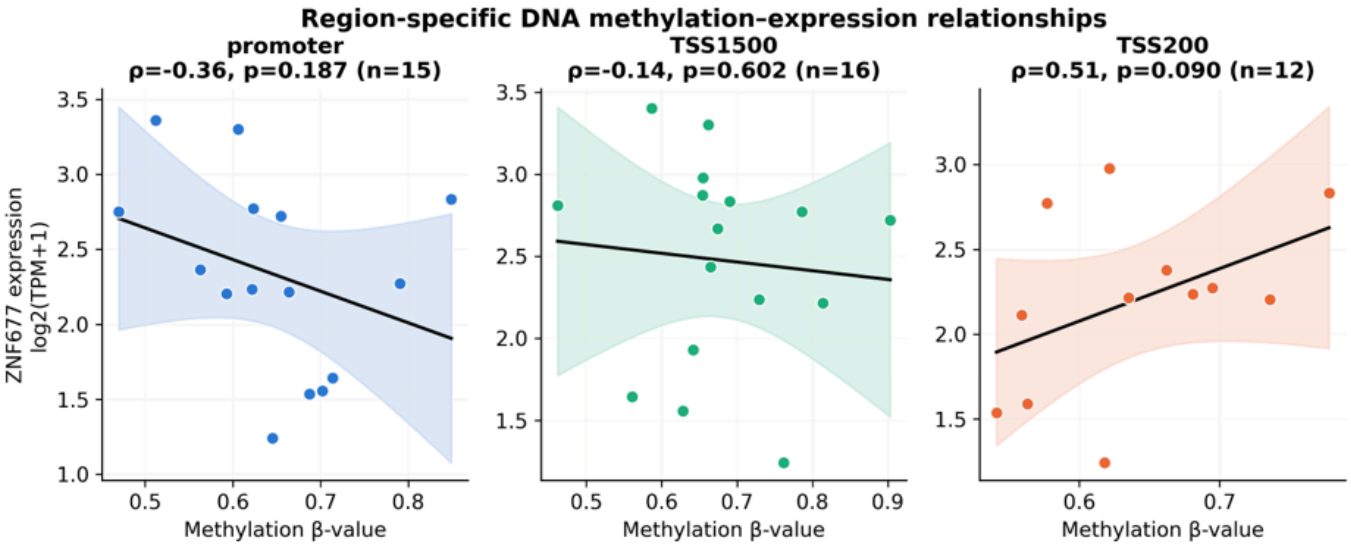


Figure 2

Region-specific DNA methylation–expression relationships. *ZNF677 expression versus mean β-value at promoter, TSS1500 and TSS200 regions with OLS fit and 95% confidence band. Promoter methylation is inversely related to expression; TSS200 shows the opposite, region-specific pattern.*

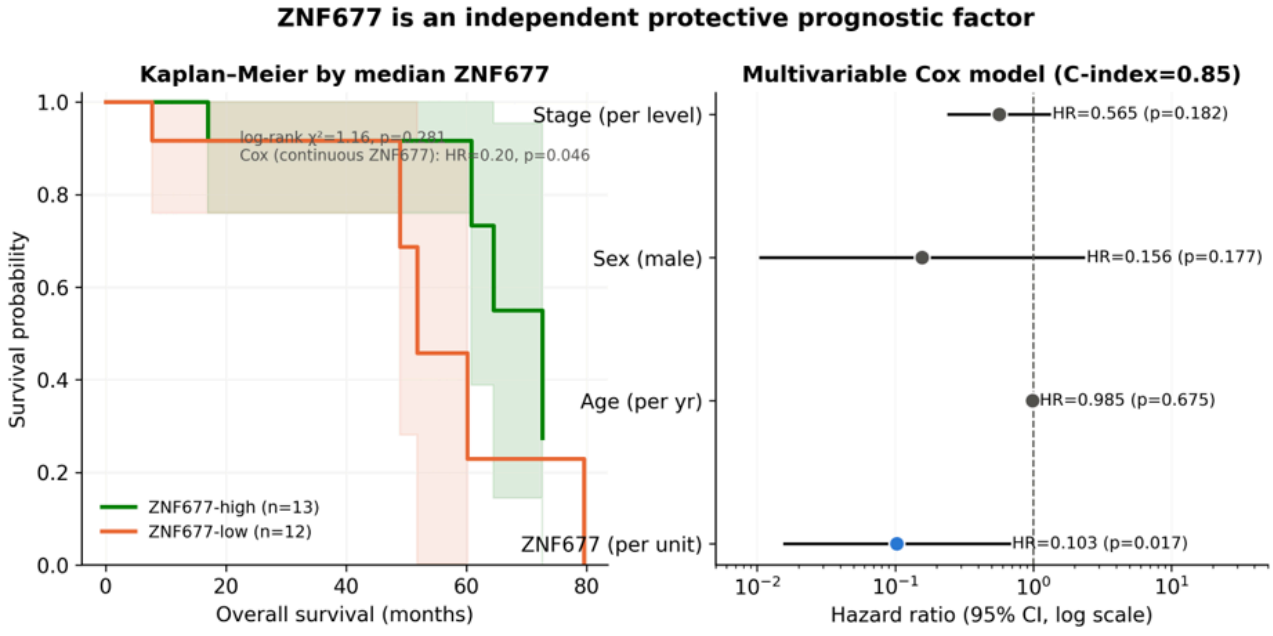


Figure 3

ZNF677 is an independent protective prognostic factor. *(Left) Kaplan–Meier overall survival by median ZNF677 with 95% confidence bands; median-split log-rank is non-significant, whereas continuous Cox is significant. (Right) Forest plot of the multivariable Cox model; continuous ZNF677 is independently protective (HR = 0.10, p = 0.017) with a C-index of 0.85.*

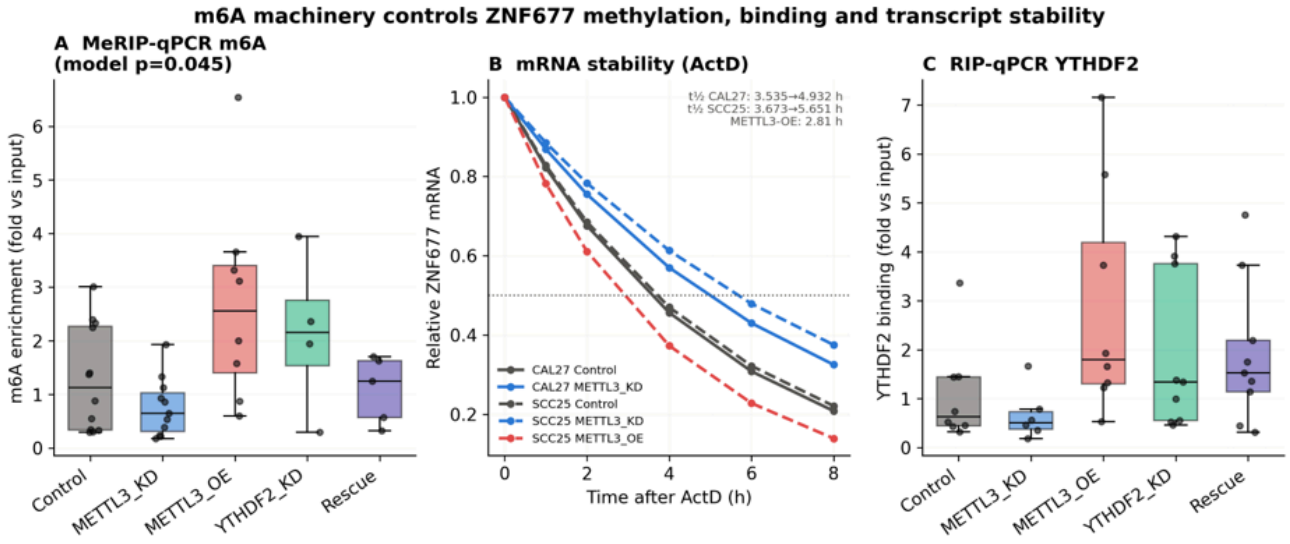


Figure 4

The METTL3–YTHDF2 axis controls ZNF677 m6A, reader binding and transcript stability. *(A) MeRIP-qPCR m6A enrichment on ZNF677 by condition (overall model p = 0.045). (B) Actinomycin-D decay curves; METTL3 knockdown extends and METTL3 overexpression shortens ZNF677 half-life (decay-rate interaction p < 0.001). (C) YTHDF2 RIP-qPCR binding, tracking METTL3 dose. Points are replicates; boxes show median and IQR.*

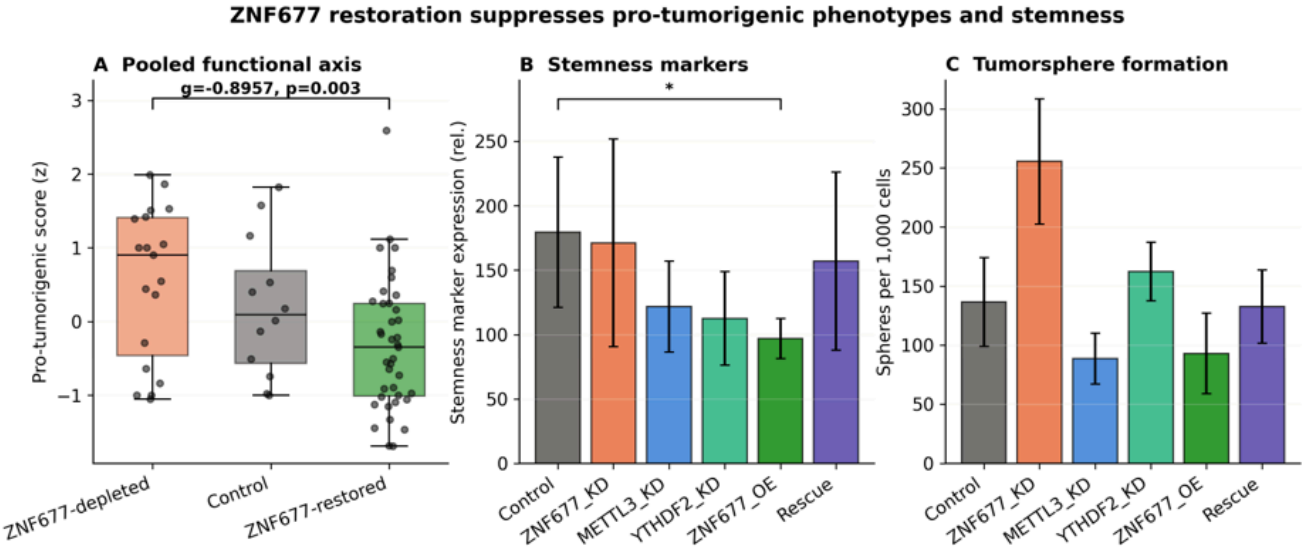


Figure 5

ZNF677 restoration suppresses pro-tumorigenic phenotypes and stemness. *(A) Pooled, z-standardised pro-tumorigenic score for ZNF677-depleting, control and ZNF677-restoring conditions; restoration lowers the score (Hedges' g = −0.90, p = 0.003). (B) Stemness-marker expression and (C) tumorsphere formation by condition (mean ± SD). *p < 0.05.*

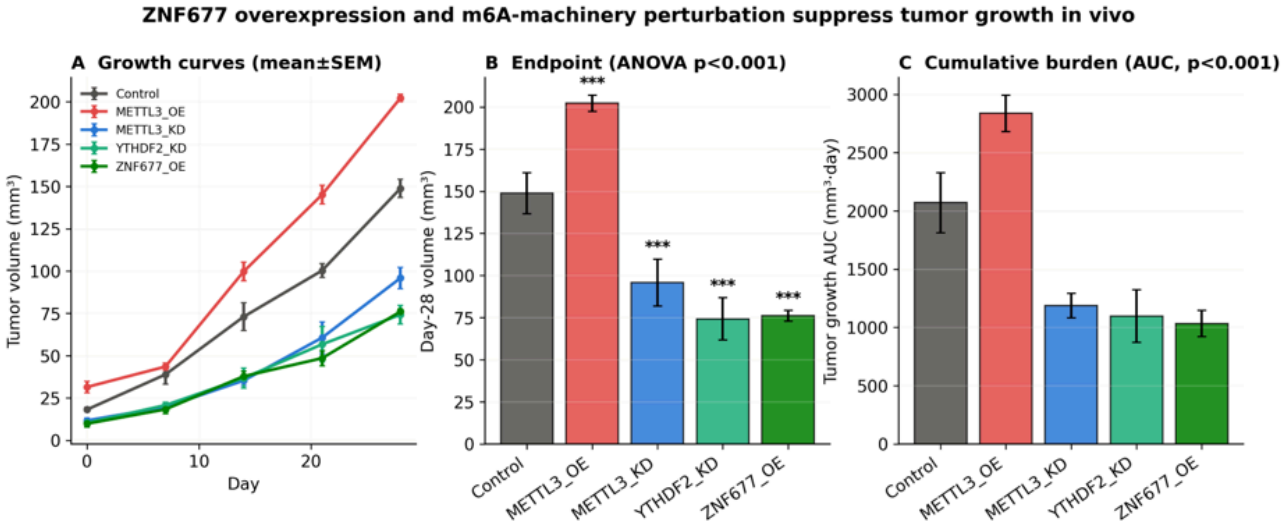


Figure 6

ZNF677 overexpression and m6A-machinery perturbation suppress tumor growth in vivo. *(A) Tumor growth curves (mean ± SEM). (B) Day-28 volumes with Tukey contrasts versus control (***p < 0.001; ANOVA p < 0.001). (C) Cumulative growth burden (area under the curve; ANOVA p < 0.001). ZNF677-restoring perturbations reduce, and METTL3 overexpression increases, tumor growth.*

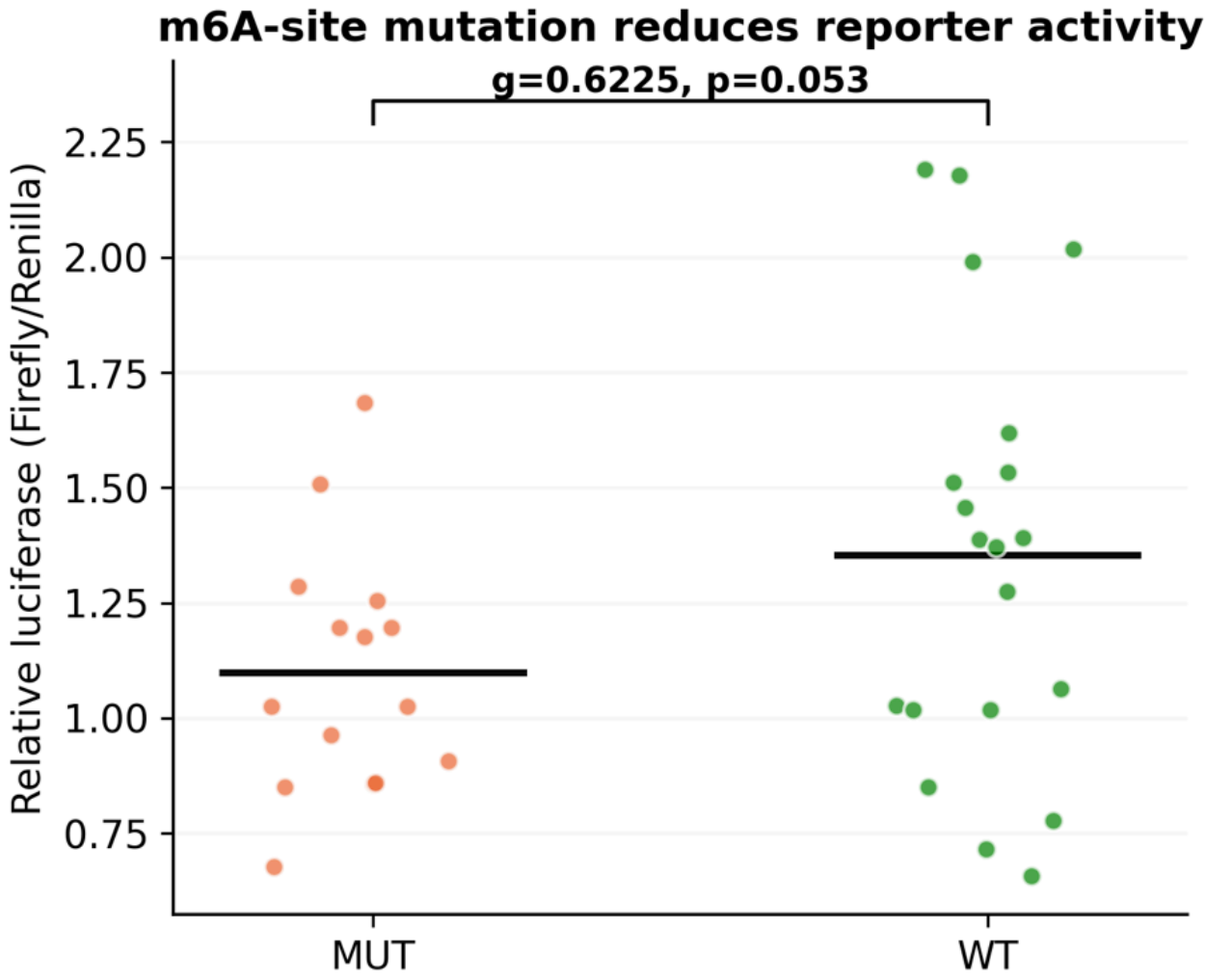


Figure 7

m6A-motif mutation reduces reporter activity. *Normalised luciferase activity for wild-type versus m6A-motif-mutant ZNF677 reporters (Hedges' g = 0.62, t-test p = 0.053). Horizontal bars indicate group means; points are replicates.*